Simulation of liquid-solid interaction using a phase-field-lattice Boltzmann method

***R. Rojas[1], and T. Takaki[2]**

[1]Mechanical and System Engineering, Graduate School of Science and Technology, Kyoto Institute of Technology, Matsugasaki, Sakyo, Kyoto 606-8585, Japan
[2]Mechanical and System Engineering, Graduate School of Science and Technology, Kyoto Institute of Technology, Matsugasaki, Sakyo, Kyoto 606-8585, Japan

*Corresponding author: rojas@kit.ac.jp

Abstract

In this study, a combination of the lattice Boltzmann method (LBM) and the phase-field method (PFM) is used for the calculation of liquid-solid two-phase flows with solidification. PFM is used as a numerical tool to capture interface topology changes of solid and the flow of liquid is solved by using LBM. The no-slip boundary condition at the liquid-solid interface is satisfied by adding a diffusive-forcing term in LBM formulation. Calculations of Poiseuille flows and flows past a circular cylinder at different Reynolds numbers confirm that the no-slip boundary condition is effectively satisfied at the diffuse liquid-solid interface. Then, the present method is applied to the calculation of two-dimensional anisotropic dendritic growth of a binary alloy under melt convection. Two cases have been studied. Initially, the solid is stationary, and then the solid is free to move under the influence of the flow. The equations of motion are solved to track the translation and rotation of the solid. Qualitative comparisons of the solidification patterns reveal that the microstructure dendritic growth is mainly affected in the direction of the fluid flow. The results obtained with the present method agree well with those obtained with other available numerical techniques.

Keywords: Liquid-solid two-phase flow, Phase-field method, Lattice Boltzmann method, Solidification

Introduction

Dendrites are common structures in the solidification of metals and alloys. They reproduce due to unstable movement of a liquid-solid interface. Dendritic solidification is governed by complex processes such as surface tension, heat transport (for pure materials) and/or concentration gradient (for alloys). Due to the importance of this phenomenon, some numerical techniques using the phase-field method (PFM) have been proposed to effectively capture the interface morphology [Karma&Rappel (1998); Ohno&Matsuura (2009)]. Other important aspect in solidification is convection. Convection plays a crucial role on crystal growth, and its effects have been studied by taking into account the effect of melt convection [Beckermann et al. (1999), Lu et al. (2003), Miller et al. (2001), Medvened et al (2006)]. In order to simulate solidification under melt convection, the aforementioned methods combine PFM to solve the phase transformation process and an appropriate method to solve the fluid flow, i.e. the solution of the Navier-Stokes equations or the lattice Boltzmann method (LBM) [Chen&Doolen (1998)]. In this studies, the solid is assumed to be stationary, so that the momentum equation for the solid is not solved.

In this study a combination of PFM proposed by Ohno&Matsuura [Ohno&Matsuura (2009)] and LBM has been used for simulation of solidification. The main advantage of this PF-LBM over others is the possibility of choosing different diffusivities in the solid and liquid parts, and therefore allowing solidification involving diffusion in solid of a binary alloy. Most importantly, the solid is allowed to move freely, and the equations of motion are solved to calculate the translational and rotational velocities. Additionally, LBM has been adopted for modeling the fluid flow due to its computational advantages related to easy programming and suitability for parallel computing.

First, the present method is applied to benchmark simulations with stationary diffuse interfaces. Poiseuille flows and flows past a circular cylinder are carried out to validate the no-slip boundary condition at the liquid-solid interface. Then, calculations of isothermal dendritic solidification under melt convection of an Al-Cu alloy are carried out. Two cases are considered to study the effect of melt convection. Initially, the solid part is considered to be stationary, and then the solid part is allowed to move with the fluid flow. The analysis of the results is based on qualitative comparisons of the differences in the solidification patterns.

Numerical Method

The present method uses the quantitative phase-field method for dilute alloy solidification [Ohno&Matsuura (2009)] and the lattice Boltzmann method with discrete forcing term [Chen&Doolen (1998)]. The interaction between solid and liquid parts is modeled by a diffuse force proposed by Beckermann et al. [Beckermann et al. (1999)]. A detailed explanation of the numerical methods is given in the following.

Phase-field method

The time evolution of the phase field, ϕ, is given by [Ohno&Matsuura (2009)]

$$a_s(\theta)^2 \partial_t \phi = \nabla \cdot \left(a_s(\theta)^2 \nabla \phi\right) - \partial_x \left[a_s(\theta) a_s'(\theta) \partial_y \phi\right] + \partial_y \left[a_s(\theta) a_s'(\theta) \partial_x \phi\right] - f'(\phi) - \lambda^* g'(\phi) u \qquad (1)$$

where $a_s(\theta)$ is a function to represent crystalline anisotropy, ϕ=-1 for liquid and ϕ=+1 for solid, $a_s'(\theta) = da_s/d\theta$, $f(\phi)$ and $g(\phi)$ are interpolating functions associated with the double-well and chemical potential, respectively, λ^* is a dimensionless parameter that controls the coupling between the phase field and the concentration field represented by the dimensionless supersaturation, u.

The time evolution of the supersaturation, u, is given by

$$\left[1 + k - (1-k) h(\phi)\right](\partial_t u + \boldsymbol{U} \cdot \nabla u)/2 = \nabla\left[D_l q(\phi) \nabla u - j_{AT}\right] + \left[1 + (1-k) u\right] \partial_t h(\phi)/2 - \nabla \cdot \boldsymbol{J} \qquad (2)$$

where k is the partition coefficient, $h(\phi)$ and $q(\phi)$ are interpolating functions, $\boldsymbol{U}$ is the fluid velocity, D_l is the liquid diffusivity, j_{AT} is the antitrapping current term, and $\boldsymbol{J}$ is a function to include noise fluctuations [Echebarria (2010)].

Lattice Boltzmann method

The lattice Boltzmann equation with single relaxation time, τ, and discrete forcing term, G_i, is given by

$$f_i(\boldsymbol{x} + \boldsymbol{c}_i \delta t, t + \delta t) = f_i(\boldsymbol{x}, t) - \frac{1}{\tau}\left[f_i(\boldsymbol{x}, t) - f_i^{eq}(\boldsymbol{x}, t)\right] + G_i(\boldsymbol{x}, t) \delta t \qquad (3)$$

where f_i is the particle velocity distribution in the ith direction, $\boldsymbol{x}$ is the position vector, $\boldsymbol{c}_i$ the discrete particle velocity, t the time, δt the time step size, f_i^{eq} is the equilibrium distribution function. The fluid density, ρ, and velocity $\boldsymbol{U}$ are given by

$$\rho = \sum_{i=0}^{Q-1} f_i \qquad (4)$$

$$\rho \boldsymbol{U} = \sum_{i=0}^{Q-1} \boldsymbol{c}_i f_i \qquad (5)$$

where Q is the number of discrete velocities. In this study, the two-dimensional nine-velocity (D2Q9) model is used in the calculations of the discrete velocity. The discrete forcing term, G_i, with second-order accuracy is given by

$$G_i = \rho W_i \left[3\frac{\boldsymbol{c}_i - \boldsymbol{u}}{c^2} + 9\frac{(\boldsymbol{c}_i \cdot \boldsymbol{u})\boldsymbol{c}_i}{c^4} \right] \cdot \boldsymbol{G} \tag{6}$$

where W_i is the weighting function related to f_i^{eq} and c the lattice velocity ($c=\delta x/\delta t=1$). $\boldsymbol{G}$ is an external force.

In the present study, effects of the gravity and other external forces are neglected. Therefore, the only force acting on the fluid flow is the one related to drag. A dissipative drag force is used to impose the no-slip boundary condition at the diffuse liquid-solid interface. It is given by [Beckermann et al. (1999)]

$$\boldsymbol{G}(\boldsymbol{x},t) = 2\rho\nu g \left(\frac{1+\phi}{2} \right)^2 (\boldsymbol{U}_S - \boldsymbol{U}) \tag{7}$$

where ν is the kinematic viscosity, g is a dimensionless constant, i.e. g = 2.757 and $\boldsymbol{U}_S$ is the solid velocity. The motion of the solid part is calculated by solving the following equations [Glowinski et al. (2001)]:

$$M_S \frac{d\boldsymbol{U}_T}{dt} = \boldsymbol{G}_S \tag{8}$$

$$\boldsymbol{I}_S \frac{d\omega_S}{dt} = \boldsymbol{T}_S \tag{9}$$

where M_S is the mass of the solid, $\boldsymbol{U}_T$ is the translational velocity of the solid, $\boldsymbol{I}_S$ is the tensor for the moment of inertia, ω_S is the angular velocity, $\boldsymbol{G}_S$ and $\boldsymbol{T}_S$ are the total force and torque acting on the solid, respectively. They are given by

$$\boldsymbol{G}_S = -\sum_{\boldsymbol{x}} \boldsymbol{G}(\boldsymbol{x},t)\Delta V \tag{10}$$

$$\boldsymbol{T}_S = -\sum_{\boldsymbol{x}} (\boldsymbol{x} - \boldsymbol{X}_S) \times \boldsymbol{G}(\boldsymbol{x},t)\Delta V \tag{11}$$

where ΔV is the volume of the computational cell and $\boldsymbol{X}_S$ is the center of mass of the solid. The velocity $\boldsymbol{U}_S$ is given by $\boldsymbol{U}_S = \boldsymbol{U}_T + \omega_S \times (\boldsymbol{x}\text{-}\boldsymbol{X}_S)$. The location of the phase field is updated with an advection equation. The advection term is discretized with the WENO fifth-order scheme.

The basic solution of the present method is illustrated as follows:

1. Solve Eqs. (1) - (2) with the explicit Euler method.
2. Solve the lattice Boltzmann equation, Eq. (3), with discrete forcing term, Eqs. (6) and (7), and obtain $\boldsymbol{U}$.
3. If necessary, calculate the motion of the solid with Eqs. (8), (9), (10) and (11) and update the location of the phase field with an advection equation.

Validation

Initially, calculations of Poiseuille flow and flows past a circular cylinder at different Reynolds numbers are carried out to validate the no-slip boundary conditions. The phase field does not

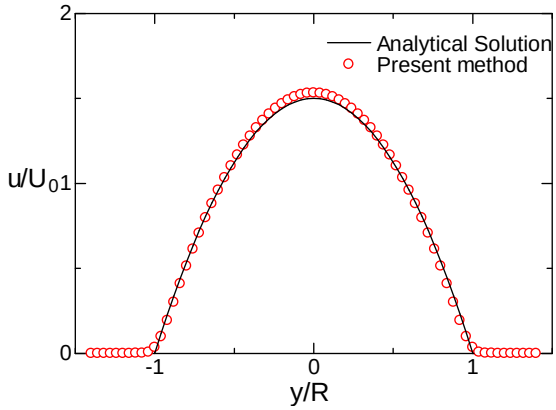

Figure 1. Velocity profile of Poiseuille flow

Table 1 Comparison of drag coefficient for steady flows past a circular cylinder

Re	10	20	40
IB-FDLBM [Rojas et al. (2011)]	2.95	2.135	1.58
Present method	3.16	2.31	1.75

Table 2 Properties of Al-Cu alloy

Diffusivity in liquid	D_l [m^2/s]	3.0×10^{-9}
Diffusivity in solid	D_s [m^2/s]	3.0×10^{-13}
Partition coefficient	k	0.14

change in these calculations and it is only used to distingue the fluid and the solid, e.g. walls or boundaries. For Poiseuille flows, the computational domain is long enough so that the predicted velocity profile corresponds to the fully developed flow. The phase field is set at ϕ=-1 at the flow region and ϕ = 1 at the top and bottom walls. Figure 1 shows a comparison of the theoretical velocity profile and the one predicted with the present method. As can be seen, both velocity profiles agree well. Moreover, the no-slip boundary condition at the top and bottom walls is effectively satisfied.

Flows past a circular cylinder are calculated using a square computational domain. The dimensions are 1600 and 1600 lattice points in the x and y directions, respectively. The left boundary condition is inlet flow at U_0, and the right, top and bottom walls are outflow boundary conditions. A circular cylinder is located at the center of the domain and the phase field is ϕ = 1, in the fluid flow ϕ = -1. Table 1 shows a comparison of the drag coefficient with other numerical results in literature [Rojas et al. (2011)]. The results obtained with the present method slightly differ from the results obtained by using an immersed boundary method. This is because in the present calculation the interface has a finite width and better agreements are expected as the interface width approaches cero.

Simulation of dendrites

In this section, numerical simulations are carried out to analyze the effect of melt convection on isothermal dendritic growth of an undercooled Al-Cu alloy. Some physical properties of an Al-Cu alloy are given in Table 2. Two cases are analyzed. In Case 1, the solid part of the alloy is stationary, i.e. $\boldsymbol{U}_S$ = 0. In case 2, the solid part is allowed to move within the fluid flow, i.e. free motion. The computational domain is shown in Fig. 2. The computational domain sizes, $W\times H$, are 1001×1001 and 2001×1001 lattice points for Cases 1 and 2, respectively. The computational domain of Case 2 is larger in the x-axis because the solid part is moving along this direction. A seed is located at (501,501) and its diameter occupies six lattice spacings. A uniform inflow at U_0 comes

from the left boundary. The right boundary is continuous outflow condition and the top and bottom walls are slip boundaries. In this study, $U_0 = 0.01$, $\tau = 1$, and $u = 0.4$.

The phase field distributions at two different instants, t_1 and t_2 are shown in Figs. 3 and 4. Figure 3 illustrates the case when the solid part is stationary. In the absence of melt convection, dendritic growth is symmetric in all directions [Ohno&Matsuura (2009)]. On the contrary, the effect of melt convection breaks the symmetrical growth morphology. As can be seen, the upstream facing parts of the alloy grow faster than those downstream orientated. These patterns agree well with other qualitative results obtained by using other numerical methods [Beckermann et al. (1999), Lu et al. (2003), Miller et al. (2001), Medvened et al (2004)].

Figure 3 shows the phase field distribution of Case 2 at t_1 and t_2. The solid part has been displaced from its initial position with $\boldsymbol{U}_S$. Despite dendritic growth seems to be symmetrical, a detailed examination revels that the rear tip grows slightly faster than the front and normal tips. This behavior is because the fluid flow enhances dendritic growth along its direction. As can be seen, the motion of the solid part is mainly related to the translational velocity of the solid. The effect of the rotational velocity is very small in this case. Therefore, calculations of dendritic growth in a shear flow are carried out to evaluate the rotation of the solid. The computational domain size is $W \times H = 1001 \times 1001$. The dimensionless velocities at top and bottom walls are -0.02 and +0.02, respectively. Periodic boundary conditions are set along the x-axis. Figures 5 (a) and (b) show the distribution of ϕ at t_1 and t_2. As can be seen, the simultaneous growth and rotation of the solid is effectively predicted. Dendritic growth is favorable along the preferable directions, and the fluid flow slightly modifies the growth in the direction perpendicular to the preferable directions.

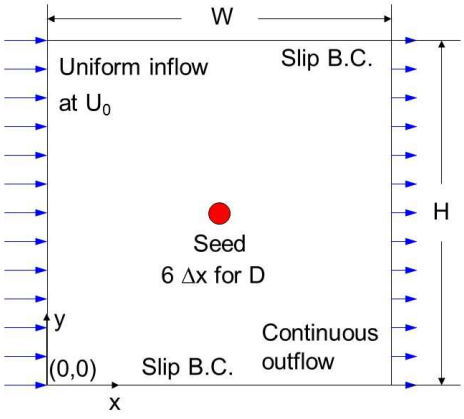

Figure 2. Computational domain for simulation of dendrites

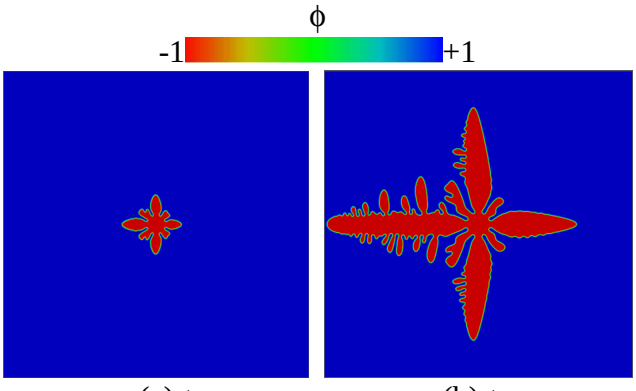

(a) t_1 (b) t_2

Figure 3. Phase field distribution, ϕ, at $U_S = 0$

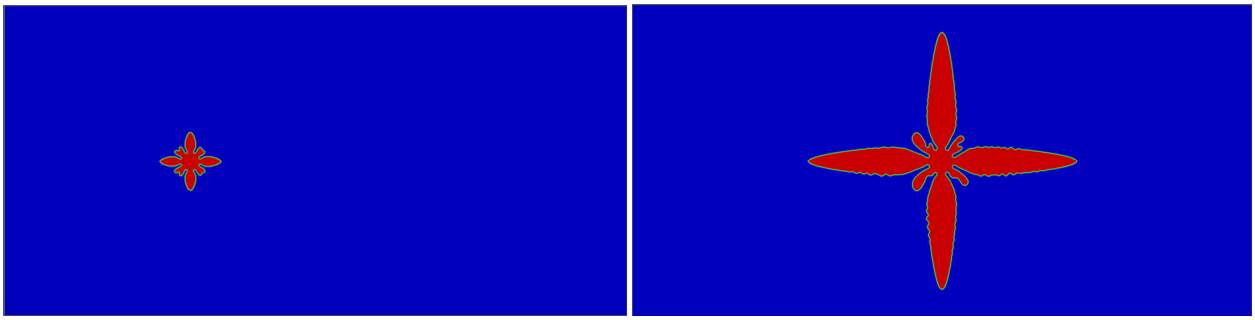

(a) t_1 (b) t_2

Figure 4. Phase field distribution, ϕ, at free motion

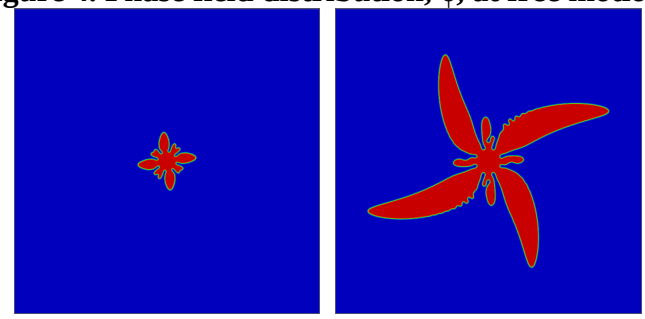

(a) t_1 (b) t_2

Figure 5. Phase field distribution, ϕ, of dendritic growth in a shear flow

Conclusions

A combination of the phase-field method and the lattice Boltzmann method was used for simulations of dendrites. Two cases were studied to analyze the effect of melt convection on dendritic growth. First, the solid part of the alloy was stationary and then it was allowed to move freely within the fluid flow. As a result, the following conclusions were obtained: (1) melt convection strongly affects the morphology of dendritic growth; it accelerates growth along its direction and (2) the motion of the solids affects dendritic growth in all directions, specially the direction of the fluid flow

References

Beckermann, C., Diepers, H.-J., Steinbach, I., Karma, A., and Tong, X. (1999) Modeling melt convection in phase-field simulations of solidification, *Journal of Computational Physics* **154**, 468-496.

Chen, S. and Doolen G.D. (1998) Lattice Boltzmann method for fluid flows, *Annual Review of Fluid Mechanics* **30**, 329-364.

Echebarria, B. (2010) Onset of sidebranching in directional solidification, *Physical Review E* **81**, 021608.

Glowinski, R., Pan, T.W., Hesla, T.I., Joseph, D.D., and Periaux, J. (2001) A fictitious domain approach to the direct simulation of incompressible viscous flow past moving rigid bodies: application to particulate flow, *Journal of Computational Physics* **169**, 363-426.

Karma, A. and Rappel W.J. (1998) Quantitative phase-field modeling of dendritic growth in two and three dimensions, *Physical Review E* **57 (4)**, 4323-4349.

Lu, Y., Beckermann, C., and Ramirez, J.C. (2005) Three-dimensional phase-field simulations of the effect of convection on free dendritic growth, *Journal of Crystal Growth* **280**, 320-334.

Miller, W., Succi, S., and Mansutti, D. (2001) Lattice Boltzmann method for anisotropic liquid-solid phase transition, *Physical Review Letters* **86 (16)**, 3578-3581.

Medvened, D., Fischaleck, T., and Kassner, K. (2006) Influence of external flows on crystal growth: Numerical investigation, *Physical Review E* **74**, 031606.

Ohno, M. and Matsumura K. (2009) Quantitative phase-field modeling for dilute alloy solidification involving diffusion in the solid, *Physical Review E* **79**, 031603.

Rojas, R., Seta, T., Hayashi, K., and Tomiyama, A. (2011) Immersed boundary-finite difference lattice Boltzmann method for liquid-solid two-phase flows, *Journal of Fluid Science and Technology* **6(6)**, 1051-1064.